J|A|C|S
ARTICLES
Published on Web 09/23/2004

A Two-Unnatural-Base-Pair System toward the Expansion of the Genetic Code

Ichiro Hirao,*,†,‡ Yoko Harada,‡ Michiko Kimoto,‡ Tsuneo Mitsui,†
Tsuyoshi Fujiwara,‡ and Shigeyuki Yokoyama*,‡,§,¶

Contribution from the Research Center for Advanced Science and Technology, The University of Tokyo, 4-6-1 Komaba, Meguro-ku, Tokyo 153-8904, Japan, Protein Research Group, RIKEN Genomic Sciences Center, 1-7-22 Suehiro-cho, Tsurumi-ku, Yokohama, Kanagawa 230-0045, Japan, Department of Biophysics and Biochemistry, Graduate School of Science, The University of Tokyo, 7-3-1 Hongo, Bunkyo-ku, Tokyo 113-0033, Japan, and RIKEN Harima Institute at SPring-8, 1-1-1 Kohto, Mikazuki-cho, Sayo, Hyogo 679-5148, Japan

Received May 13, 2004; E-mail: ihirao@postman.riken.jp; yokoyama@biochem.s.u-tokyo.ac.jp

Abstract: Toward the site-specific incorporation of amino acid analogues into proteins, a two-unnatural-base-pair system was developed for coupled transcription−translation systems with the expanded genetic code. A previously designed unnatural base pair between 2-amino-6-(2-thienyl)purine (denoted by **s**) and pyridin-2-one (denoted by **y**) was used for the site-specific incorporation of **y**TP into RNA opposite **s** in templates by T7 RNA polymerase. For the site-specific incorporation of **s**TP into RNA, a newly developed unnatural base, imidazolin-2-one (denoted by **z**), is superior to **y** as a template base for pairing with **s** in T7 transcription. The combination of the **s**-**y** and **s**-**z** pairs provides a powerful tool to prepare both **y**-containing mRNA and **s**-containing tRNA for efficient coupled transcription−translation systems, in which the genetic code is expanded by the codon−anticodon interactions mediated by the **s**-**y** pair. In addition, the nucleoside of **s** is strongly fluorescent, and thus the **s**-**z** pair enables the site-specific fluorescent labeling of RNA molecules. These unnatural-base-pair studies provide valuable information for understanding the mechanisms of replication and transcription.

Introduction

The creation of unnatural base pairs for the expansion of the genetic alphabet and code allows us to incorporate various unnatural, functional components into nucleic acids and proteins at desired positions.[1−3] For this purpose, unnatural base pairs that have exclusive selectivity and work together with the natural A−T(U) and G−C pairs in replication, transcription, and translation are required.

Previous efforts pursued the use of unnatural base pairs, such as isoG and isoC, with hydrogen-bonding patterns different from those of the natural Watson−Crick base pairs.[4−6] These unnatural base pairs functioned with moderate selectivity in replication and transcription, and the isoG-isoC pair was applied to a cell-free translation system for the incorporation of 3-iodotyrosine into a peptide.[7] In this translation system, however, the mRNA and tRNA containing the unnatural bases were prepared by laborious chemical synthesis. Although the isoG can be incorporated into RNA opposite isoC by T7 transcription, the isoC incorporation into RNA is not useful, due to the instability of isoCTP and the misincorporation of T by the tautomerization of isoG.[5] On the other hand, recent studies of unnatural hydrophobic base analogues, such as 4-methylbenzimidazole and 2,4-difluorotoluene, revealed that the steric effects between pairing bases are important for DNA replication.[8,9] Although hydrophobic base pairs are also potential candidates for unnatural base pairs,[10,11] there have been no reports on transcription mediated by hydrophobic base pairs. However, these studies have shed light on several factors, such as hydrogen bonding, steric interactions, base-stacking, and hydrophobicity, as the design principles for the further development of unnatural base pairs.[12,13]

† Research Center for Advanced Science and Technology, The University of Tokyo.
‡ RIKEN Genomic Sciences Center.
§ Department of Biophysics and Biochemistry, Graduate School of Science, The University of Tokyo.
¶ RIKEN Harima Institute at SPring-8.

(1) Benner, S. A.; Burgstaller, P.; Battersby, T. R.; Jurczyk, S. In *The RNA World*, 2nd ed.; Gesteland, R. F., Cech, T. R., Atkins, J. F., Eds.; Cold Spring Harbor Laboratory Press: Cold Spring Harbor, NY, 1999; p 163.
(2) Henry, A. A.; Romesberg, F. E. *Curr. Opin. Chem. Biol.* **2003**, *7*, 727.
(3) Bergstrom, D. E. *Chem. Biol.* **2004**, *11*, 18.
(4) Piccirilli, J. A.; Krauch, T.; Moroney, S. E.; Benner, S. A. *Nature* **1990**, *343*, 33.
(5) Switzer, C. Y.; Moroney, S. E.; Benner, S. A. *Biochemistry* **1993**, *32*, 10489.
(6) Horlacher, J.; Hottiger, M.; Podust, V. N.; Hübscher, U.; Benner, S. A. *Proc. Natl. Acad. Sci. U.S.A.* **1995**, *92*, 6329.
(7) Bain, J. D.; Switzer, C.; Chamberlin, A. R.; Benner, S. A. *Nature* **1992**, *356*, 537.
(8) Moran, S.; Ren, R. X.-F.; Kool, E. T. *Proc. Natl. Acad. Sci. U.S.A.* **1997**, *94*, 10506.
(9) Morales, J. C.; Kool, E. T. *Nat. Struct. Biol.* **1998**, *5*, 950.
(10) McMinn, D. L.; Ogawa, A. K.; Wu, Y.; Liu, J.; Schultz, P. G.; Romesberg, F. E. *J. Am. Chem. Soc.* **1999**, *121*, 11585.
(11) Wu, Y.; Ogawa, A. K.; Berger, M.; McMinn, D. L.; Schultz, P. G.; Romesberg, F. E. *J. Am. Chem. Soc.* **2000**, *122*, 7621.
(12) Kool, E. T. *Curr. Opin. Chem. Biol.* **2000**, *4*, 602.

10.1021/ja047201d CCC: $27.50

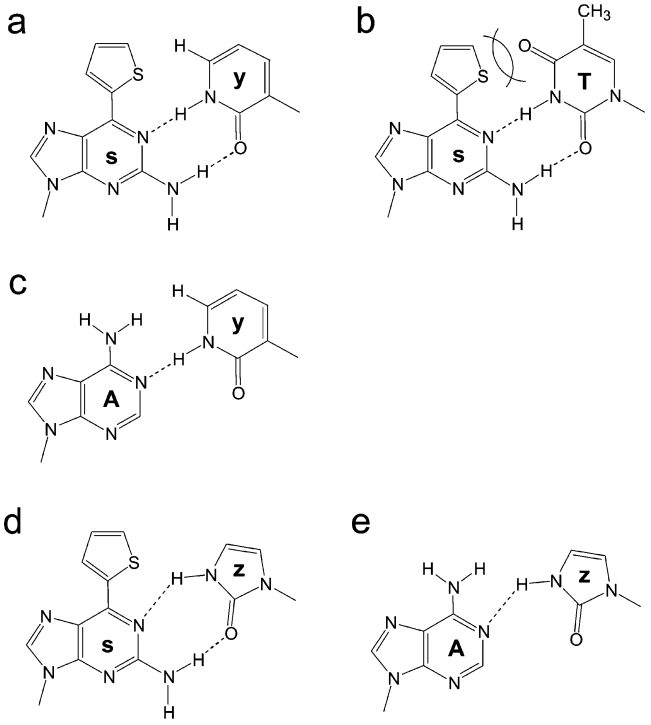

Figure 1. Cognate unnatural base pairs and their noncognate pairs: the cognate **s**-**y** (a), noncognate **s**-T (b) and A-**y** (c), cognate **s**-**z** (d), and noncognate A-**z** (e) pairs.

By combining the concepts of hydrogen-bonding patterns and steric interactions, we previously developed an unnatural base pair between 2-amino-6-(2-thienyl)purine (denoted by **s**) and pyridin-2-one (denoted by **y**) (Figure 1a).[14,15] The bulky thienyl group of **s** effectively excludes the pairing with natural bases, enabling the specific pairing between **s** and **y** (Figure 1a,b). The **s**-**y** pair functions specifically in DNA duplex formation, replication, translation, and especially transcription. The substrate of **y** (denoted by **y**TP) can be site-specifically incorporated by T7 RNA polymerase into RNA opposite **s** in templates, and the incorporation fidelity of **y** opposite **s** is more than 95%. Using the **s**-**y** pair, we created an extra codon−anticodon interaction and achieved the site-specific incorporation of an amino acid analogue, 3-chlorotyrosine, into the human Ha-Ras protein by coupled transcription−translation in a cell-free system[15] (see Figure 4).

Although this cell-free coupled transcription−translation system has the potential for the efficient synthesis of artificial proteins with amino acid analogues, the **s**-**y** pair still has some shortcomings for practical uses. In this system, the tRNA molecule containing **s** in the anticodon had to be prepared by a laborious method combining chemical synthesis and enzymatic ligation.[15] This is because of the unidirectional complementarity of the **s**-**y** pair; the incorporation of **s** into RNA opposite **y** is less selective than that of **y** opposite **s** in T7 transcription. The unnatural base **s** has the bulky thienyl group, which prevents pairing with the natural bases. On the other hand, **y** has no such functional group. Thus, the substrates of the natural purines, especially A, are partially incorporated into RNA opposite **y** in templates (Figure 1c), and the incorporation fidelity of **s** opposite **y** was reduced by 70−80%. Consequently, this insufficient selectivity of **s** incorporation opposite **y** hampers the transcriptional preparation of RNA fragments containing **s**.

To overcome this problem with the **s**-**y** pair, we designed imidazolin-2-one (denoted by **z**) as an efficient pairing partner of **s** (Figure 1d). The shape fitting between the five-membered ring of **z** and **s** was expected to be better than that between the six-membered ring of **y** and **s**. Although the hydrogen bonding between **s** and **z** is less effective than that between **s** and **y**, both the hydrogen bonding and shape fitting in the noncognate G-**z** and A-**z** pairs (Figure 1e) should be much less effective than those in the G-**y** and A-**y** pairs (Figure 1c). As compared to the six-membered ring of **y**, the loose fitting of the five-membered ring of **z** with the natural purines may not effectively exclude water molecules on the pairing surface of A or G in replication.[16] Thus, the **s**-**z** pairing was expected to be more selective than the **s**-**y** pairing. Here, we compare the potential of the **s**-**z** pairing to the **s**-**y** pairing through experiments in transcription and replication, and by the thermal stability of the **s**-**z** pair in duplex DNA. We also report the synthesis of tRNA containing **s** in the anticodon, by T7 transcription mediated by the **s**-**z** pairing, and discuss the two-unnatural-base-pair system for the expansion of the genetic code.

Results and Discussion

The 2′-deoxyribonucleoside of **z** was synthesized by the glycosidation of 1-chloro-2-deoxy-3,5-di-*O*-toluoyl-α-D-erythropentofuranose and trimethylsilylated imidazolin-2-one with $SnCl_4$ (Scheme 1). After deprotection of the toluoyl groups, both the β-isomer and α-isomer were isolated with total yields of 19 and 24%, respectively. These structures were confirmed by ^{1}H NMR and mass spectrometry; the β-isomer generated NOEs between H1′ and H4′, and H1′ and H2″, unlike the α-isomer (see Supporting Information). Furthermore, the ^{1}H NMR spectrum of the β-isomer was identical to that of the product obtained by a different synthesis route, in which the β-isomer was derived from the β-D-ribonucleoside of **z**[17] by deoxygenation of the 2′-hydroxy group.[18] For DNA chemical synthesis, the base moiety was protected with a diphenylcarbamoyl group, and then the nucleoside was converted to the amidite. The stability of the **z** nucleoside in DNA fragments, under the deprotection conditions after DNA synthesis, was tested using the trimer, d(T**z**T), and no decomposition was observed after treatment with concentrated NH_4OH at 55 °C for 6 h. DNA templates (35-mer and 104-mer) containing **z** were synthesized. The coupling efficiency of the amidite was >98% on a DNA synthesizer (Applied Biosystems). Furthermore, the 2′-deoxyribonucleoside of **z** was converted to the nucleoside 5′-triphosphate (d**z**TP), to function as a substrate in replication.

First, we examined the thermal stability of a duplex DNA (12-mer) containing the **s**-**z** pair, to assess the specificity of the unnatural base pair formation. The DNA duplex containing the **s**-**z** pair (T_m = 42.3 °C) was as stable as that containing the **s**-**y** pair (T_m = 42.9 °C), even though the stacking ability of the five-membered ring of **z** might be inferior to that of the six-

(13) Kool, E. T. *Annu. Rev. Biophys. Biomol. Struct.* **2001**, *30*, 1.
(14) Fujiwara, T.; Kimoto, M.; Sugiyama, H.; Hirao, I.; Yokoyama, S. *Bioorg. Med. Chem. Lett.* **2001**, *11*, 2221.
(15) Hirao, I.; Ohtsuki, T.; Fujiwara, T.; Mitsui, T.; Yokogawa, T.; Okuni, T.; Nakayama, H.; Takio, K.; Yabuki, T.; Kigawa, T.; Kodama, K.; Yokogawa, T.; Nishikawa, K.; Yokoyama, S. *Nat. Biotechnol.* **2002**, *20*, 177.
(16) Kool, E. T.; Morales, J. C.; Guckian, K. M. *Angew. Chem., Int. Ed.* **2000**, *39*, 990.
(17) Haines, D. R.; Leonard, N. J.; Wiemer, D. F. *J. Org. Chem.* **1982**, *47*, 474.
(18) Ishikawa, M.; Hirao, I.; Yokoyama, S. *Tetrahedron Lett.* **2000**, *41*, 3931.

Scheme 1. Synthesis of the Amidite and the Triphosphate of **z**[a]

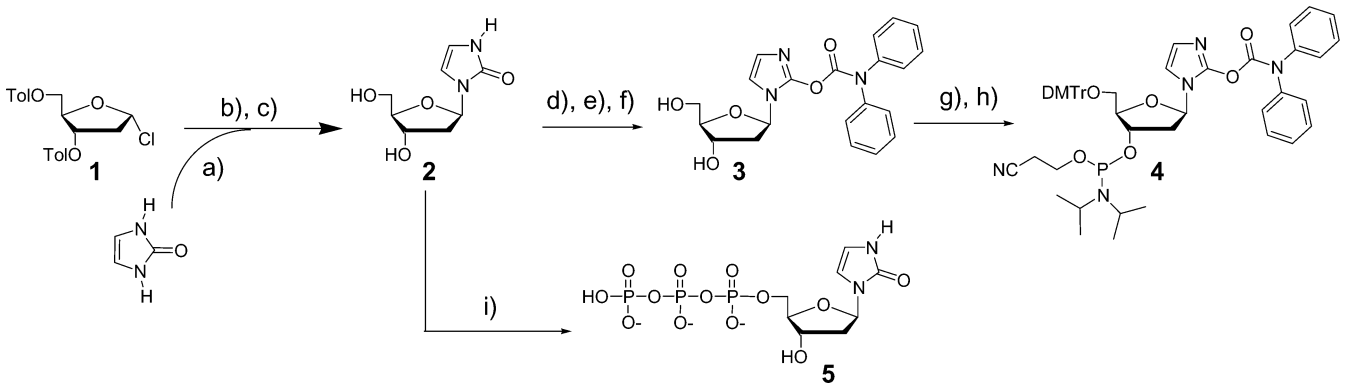

[a] Reagents: (a) hexamethyldisilazane, ammonium sulfate, dichloroethane; (b) $SnCl_4$, acetonitrile; (c) methanolic ammonia, β-isomer (19%) and α-isomer (24%) from **1**; (d) 1,3-dichloro-1,1,3,3-tetraisopropyldisiloxane, DMF, pyridine, 78%; (e) diphenylcarbamoyl chloride, $^{i}Pr_2EtN$, pyridine, 60%; (f) tetrabutylammonium fluoride, THF, 96%; (g) 4,4′-dimethoxytrityl chloride, pyridine, 86%; (h) $ClP(N\text{-}^{i}Pr_2)(OCH_2CH_2CN)$, $^{i}Pr_2EtN$, THF, 86%; (i) $POCl_3$, proton sponge, $PO(OCH_3)_3$, then tri-*n*-butylamine, bis(tributylammonium)pyrophosphate, DMF. Abbreviations: DMTr, dimethoxytrityl; ^{i}Pr, isopropyl; Tol, toluoyl.

Table 1. Steady-State Kinetic Parameters for Insertion of Single Nucleotides into a Template−Primer Duplex by the Exonuclease-Deficient Klenow Fragment

primer 1 5'-ACTCACTATAGGGAGGAAGA
template 1 3'-TATTATGCTGAGTGATATCCCTCCTTCT**N**TCTCGA

primer 2 5'-ACTCACTATAGGGAGCTTCT
template 2 3'-TATTATGCTGAGTGATATCCCTCGAAGA**N**AGAGCT

entry	primer–template set	template (N)	nucleoside triphosphate	K_m (μM)	V_{max} (%·min^{-1})[a]	V_{max}/K_m (%·min^{-1}·M^{-1})
1	1	**s**	**z**	600 (210)[b]	34 (6)	5.7×10^4
2	1	A	**z**	1800 (500)	5.0 (1.9)	2.8×10^3
3	1	G	**z**	770 (540)	2.1 (1.3)	2.7×10^3
4	1	C	**z**	nd[c]	nd	
5	1	T	**z**	900 (700)	0.065 (0.030)	7.2×10^1
6	2	**z**	**s**	95 (30)	55 (17)	5.8×10^5
7	2	**z**	A	540 (140)	8.9 (2.4)	1.6×10^4
8	2	**z**	G	270 (170)	0.57 (0.20)	2.1×10^3
9	2	**z**	C	nd	nd	
10	2	**z**	T	58 (56)	0.041 (0.027)	7.1×10^2
11	1	**s**	**y**	170 (60)	10 (4)	5.9×10^4
12	1	A	**y**	220 (90)	11 (3)	5.0×10^4
13	1	G	**y**	140 (30)	1.1 (0.3)	7.9×10^3
14	1	C	**y**	nd	nd	
15	1	T	**y**	nd	nd	
16	2	**y**	**s**	68 (19)	69 (11)	1.0×10^6
17	2	**y**	A	370 (190)	56 (12)	1.5×10^5
18	2	**y**	G	310 (110)	4.2 (1.0)	1.4×10^4
19	2	**y**	C	1000 (300)	0.19 (0.01)	1.9×10^2
20	2	**y**	T	4.8 (4.9)	0.78 (0.39)	1.6×10^5
21	1	A	T	1.5 (0.5)	1.8 (0.3)	1.2×10^6
22	1	A	C	2000 (1500)	1.7 (0.7)	8.5×10^2
23	2	T	A	3.9 (1.3)	11 (2)	2.8×10^6
24	2	C	A	490 (80)	2.9 (0.9)	5.9×10^3

[a] The values were normalized to the enzymatic concentration (20 nM) for the various enzyme concentrations used. [b] Standard deviations are given in parentheses. [c] nd, no inserted products were detected after an incubation for 20 min with 2100 or 2400 μM nucleoside triphosphate and 45 nM enzyme.

membered ring of **y**. Interestingly, the selectivity of the **s**-**z** pair was significantly improved, and the duplex DNA containing the **s**-**z** pair (T_m = 42.3 °C) was stabilized by 2.8−6.8 °C relative to the mispairs between **z** and the natural purine bases (T_m's = 35.5 and 39.5 °C for the A-**z** and G-**z** pairs, respectively). In contrast, the stability of the duplex DNA containing the noncognate G-**y** pair (T_m = 43.1 °C) was as high as that of the duplex DNA containing the **s**-**y** pair (T_m = 42.9 °C), although the **s**-**y** pair was more stable than the A-**y** pair (T_m = 36.2 °C).

Before we tested the **s**-**z** pair in transcription, we examined the potential of the **s**-**z** pairing in replication, since the determination of the kinetic parameters of base pairings in replication is much easier than that in transcription, and the structures and mechanisms between DNA polymerases and RNA polymerases are quite similar.[19−21] Thus, the selectivity of the **s**-**z** pairing against the noncognate pairings was compared with

(19) Sousa, R.; Chung, Y. J.; Rose, J. P.; Wang, B.-C. *Nature* **1993**, *364*, 593.
(20) Cheetham, G. M. T.; Jeruzalmi, D.; Steitz, T. A. *Nature* **1999**, *399*, 80.

that of the **s**-**y** pairing by the steady-state kinetics of single-nucleotide insertion experiments. The exonuclease-deficient Klenow fragment of *Escherichia coli* DNA polymerase I was used with combinations between nucleoside triphosphates and double-stranded templates (35-mer; template 1 and template 2) with a ^{32}P-labeled primer (20-mer), in which various bases in the templates were adjacent to the 3′ end of the primer (Table 1).

The selectivity of the **s**-**z** pairing was greatly improved (Table 1, entries 1−10), in comparison to that of the **s**-**y** pairing (Table 1, entries 11−20), and the efficiencies of the **s**-**z** pairing (Table 1, entries 1 and 6) were as high as those of the **s**-**y** pairing (Table 1, entries 11 and 16). The incorporation efficiency of d**z**TP opposite **s** was 20- and 21-fold higher than those of d**z**TP opposite A and G, respectively (Table 1, entries 1−3), and the incorporation efficiency of d**s**TP opposite **z** was 36- and 276-fold higher than those of dATP and dGTP, respectively, opposite **z** (Table 1, entries 6−8). In contrast, the incorporation efficiency of d**y**TP opposite **s** was only 1.2- and 7-fold higher than those of d**y**TP opposite A and G, respectively (Table 1, entries 11−13), and the incorporation efficiency of d**s**TP opposite **y** was 7- and 71-fold higher than those of dATP and dGTP, respectively, opposite **y** (Table 1, entries 16−18). In addition, the noncognate pairings of **z** with natural pyrimidines (Table 1, entries 4, 5, 9, and 10) showed much lower efficiencies than the **s**-**z** pairing (Table 1, entries 1 and 6). Unexpectedly, T was efficiently incorporated opposite **y** ($V_{max}/K_m = 1.6 \times 10^5$, Table 1, entry 20), and the T incorporation opposite **z** ($V_{max}/K_m = 7.1 \times 10^2$) was rarely observed (Table 1, entry 10). Thus, the **s**-**z** pair showed highly exclusive selectivity in the single-nucleotide insertion by the DNA polymerase. Interestingly, the pairing between d**s**TP and **z** in the template was favored over that between d**z**TP and **s** in the template; the incorporation of d**s**TP opposite **z** ($V_{max}/K_m = 5.8 \times 10^5$) was 10-fold more efficient than the incorporation of d**z**TP opposite **s** ($V_{max}/K_m = 5.7 \times 10^4$). This suggests that **z** has potential as a template base, rather than a triphosphate substrate.

Since the **s**-**z** pair showed high selectivity in replication and thermal selectivity in duplex DNA, we examined its pairing selectivity in transcription. The incorporation of **s**TP into RNA was carried out by T7 RNA polymerase, using DNA templates (temp35**z**, temp35**y**, temp35C, and temp35T) in which **z**, **y**, C, or T was located at a complementary site corresponding to position 11 in the transcripts (Figure 2a). The internally labeled transcripts were analyzed on a gel (Figure 2b), and then were fully digested to nucleoside 3′-phosphates for a nucleotide-composition analysis on a 2D-TLC plate (Figure 2c). Afterward, the amount of each nucleoside 3′-phosphate was quantified (Table 2). Since [α-^{32}P]UTP was used for labeling in transcription, the 3′-phosphates of the nucleotides that became the 5′-neighbor of U in the transcripts were labeled. Thus, the digestion of the transcripts by RNase T_2 generated three labeled Cp's, one labeled Up, and a labeled nucleotide at position 11.

After 3 h of transcription, the relative yields of the 17-mer transcripts (Figure 2b, lanes 3 and 6) were 40−60% relative to those obtained from the natural templates (N = T or C) with the natural NTPs (data not shown), although truncated transcripts (10-mer and 11-mer in Figure 2b) from temp35**y** and temp35**z**

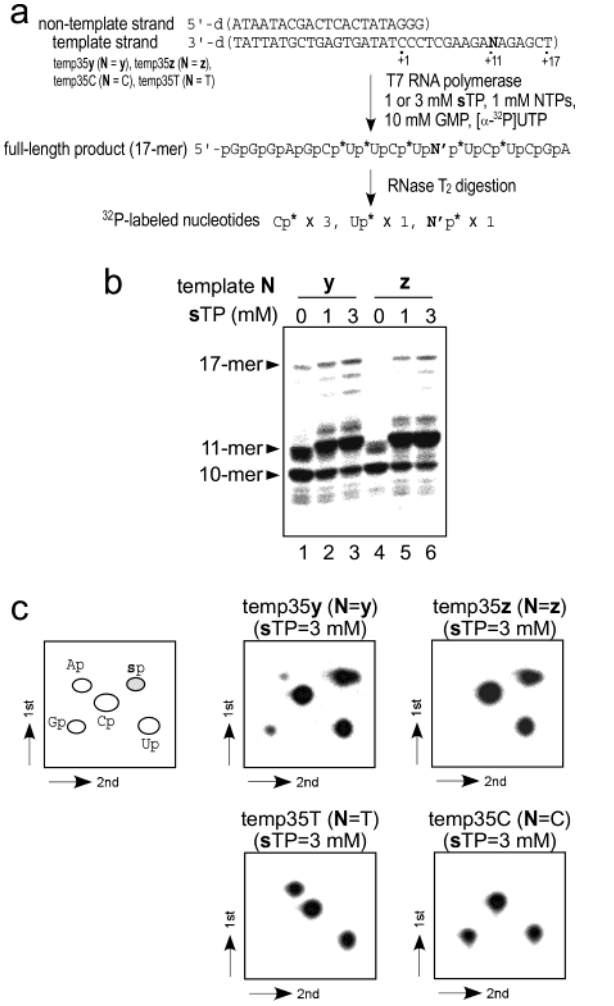

Figure 2. Unnatural T7 transcription employing **s**-**z** pairing. Schemes of the experiments (a). Gel electrophoresis of transcripts using the templates (N = **y** or **z**) in the presence or in the absence of the substrate of **s** (**s**TP) (b). 2D-TLC for nucleotide-composition analyses of transcripts, isolated by the gel electrophoresis shown in panel b (lanes 3 and 6), and the transcripts from templates (N = T or C) (c). The quantitative data are shown in Table 2.

were observed. As shown in Figure 2b,c, the **s** incorporation opposite **z** showed higher selectivity than that opposite **y** in T7 transcription. No 17-mer transcript was generated from temp35**z** in the absence of **s**TP (Figure 2b, lane 4). However, in the **s**-**y** pairing, even in the absence of **s**TP, the full-length transcript (17-mer) was produced with temp35**y** (Figure 2b, lane 1).

The nucleotide-composition analysis of the 17-mer transcripts confirmed the high selectivity of the **s** incorporation opposite **z** in transcription (Figure 2c and Table 2). Among the purine substrates, only a spot corresponding to **s**, which originated from the incorporation opposite **z**, was observed in the transcription using temp35**z** (Figure 2c, N = **z**, and Table 2, entries 1 and 2), and no misincorporation of **s**TP opposite T or C occurred in the transcription using temp35T and temp35C (Figure 2c, N = T and C, and Table 2, entries 6, 7, 9, and 10). In contrast, even in the presence of a 3-fold excess of sTP (3 mM) relative to the natural NTPs (1 mM), a few misincorporations of GTP and ATP opposite **y** were observed in the transcription using temp35**y** (Figure 2c, N = **y**, and Table 2, entry 4). The specificity of the **s** incorporation opposite **z** was more than 96%

(21) Temiakov, D.; Patlan, V.; Anikin, M.; McAllister, W. T.; Yokoyama, S.; Vassylyev, D. G. *Cell* **2004**, *116*, 381.

Table 2. Nucleotide Composition Analysis of T7 Transcripts

entry	template	[α-^{32}P] NTP	**s**TP (mM)	composition of nucleotides incorporated as 5′ neighbor of U or A or G[a] Ap	Gp	Cp	Up	sp
1	temp35**z**	UTP	1	0.04[b] [0][c] (<0.01)[d]	0.02 [0] (<0.01)	2.92 [3] (0.06)	1.08 [1] (0.04)	0.95 [1] (0.02)
2	temp35**z**	UTP	3	0.02 [0] (<0.01)	0.01 [0] (<0.01)	2.96 [3] (0.08)	1.05 [1] (0.06)	0.96 [1] (0.02)
3	temp35**y**	UTP	1	0.07 [0] (0.01)	0.18 [0] (0.02)	2.98 [3] (0.06)	1.07 [1] (0.03)	0.71 [1] (0.08)
4	temp35**y**	UTP	3	0.04 [0] (<0.01)	0.09 [0] (<0.01)	2.98 [3] (0.03)	1.06 [1] (0.01)	0.82 [1] (0.01)
5	temp35T	UTP	0	1.00 [1] (<0.01)	<0.01 [0] (<0.01)	2.97 [3] (<0.01)	1.03 [1] (<0.01)	nd[e] [0]
6	temp35T	UTP	1	1.00 [1] (0.02)	<0.01 [0] (<0.01)	2.97 [3] (0.03)	1.02 [1] (0.02)	<0.01 [0] (<0.01)
7	temp35T	UTP	3	0.99 [1] (0.04)	<0.01 [0] (<0.01)	2.98 [3] (0.04)	1.03 [1] (<0.01)	<0.01 [0] (<0.01)
8	temp35C	UTP	0	0.01 [0] (<0.01)	0.99 [1] (0.02)	3.00 [3] (0.01)	1.00 [1] (0.01)	nd [0]
9	temp35C	UTP	1	0.01 [0] (<0.01)	1.00 [1] (0.04)	2.98 [3] (0.04)	1.02 [1] (<0.01)	<0.01 [0] (<0.01)
10	temp35C	UTP	3	<0.01 [0] (<0.01)	0.99 [1] (<0.01)	2.99 [3] (0.02)	1.02 [1] (0.02)	<0.01 [0] (<0.01)
11	tRNA104**z**	ATP	3	5.12 [5] (0.12)	5.99 [6] (0.12)	5.88 [6] (0.07)	0.04 [0] (<0.01)	0.96 [1] (0.05)
12	tRNA104T	ATP	0	6.13 [6] (0.08)	5.90 [6] (0.08)	5.98 [6] (0.07)	0.99 [1] (0.01)	nd [0]
13	tRNA104T	ATP	3	5.98 [6] (0.07)	5.98 [6] (0.08)	5.96 [6] (0.09)	0.99 [1] (0.02)	0.09 [0] (0.05)
14	tRNA104**z**	GTP	3	5.12 [5] (0.04)	6.79 [7] (0.06)	6.16 [6] (0.05)	1.97 [2] (0.03)	0.05 [0] (<0.01)
15	tRNA104T	GTP	0	5.01 [5] (0.01)	6.84 [7] (0.04)	6.10 [6] (0.05)	2.16 [2] (0.01)	nd [0]
16	tRNA104T	GTP	3	5.10 [5] (0.05)	6.95 [7] (0.06)	6.01 [6] (0.11)	2.00 [2] (0.04)	0.05 [0] (0.04)

[a] Composition of nucleotides incorporated as 5′ neighbor of U (Entries 1−10) or A (Entries 11−13) or G (Entries 14−16), as shown in Figures 2 and 3. [b] The values were determined using the following formula: (radioactivity of each nucleotide)/[total radioactivity of all nucleotides (3′-monophosphates)] × (total number of nucleotides at 5′ neighbor of [α-^{32}P]NTP). [c] The theoretical number of each nucleotide is shown in brackets. [d] Standard deviations are shown in parentheses. [e] Not detected.

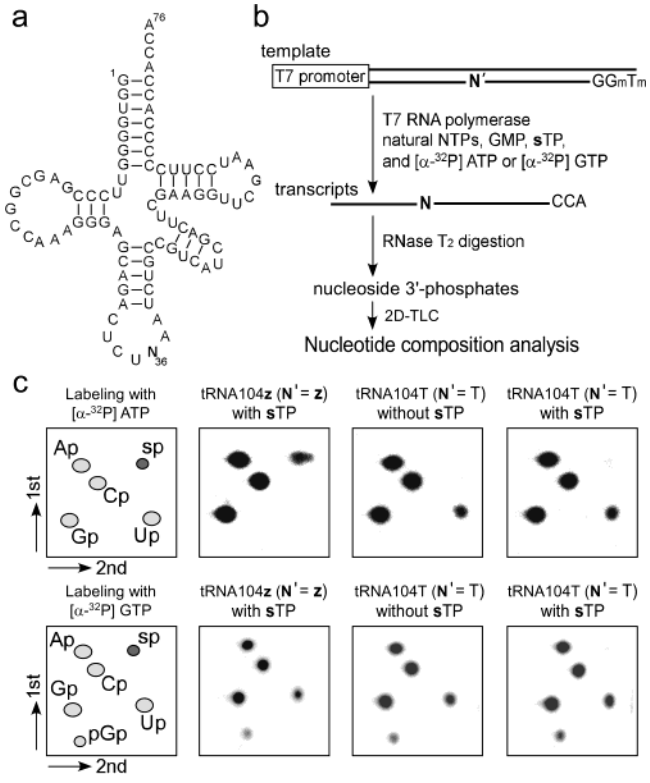

Figure 3. tRNA synthesis by T7 transcription mediated by the **s**-**z** pairing. The secondary structure of *E. coli* suppressor tRNA^{Tyr}, in which the base at position 36 is **s** or A (a). Preparation of the tRNA containing **s** at position 36 by T7 transcription (b). 2D-TLC for nucleotide-composition analyses of tRNA transcripts labeled with [α-^{32}P]ATP or [α-^{32}P]GTP (c). The quantitative data are shown in Table 2.

in the transcription using the combination of 3 mM **s**TP and 1 mM natural NTPs (Table 2, entry 2).

We synthesized tRNA containing **s** in the anticodon by T7 transcription, using a DNA template containing **z**. The sequence of *E. coli* suppressor tRNA^{Tyr} was employed (Figure 3a). This tRNA was specifically aminoacylated with an amino acid analogue, 3-iodotyrosine, by an *E. coli* tyrosyl-tRNA synthetase variant (V35C195), but was not aminoacylated with natural amino acids by the eukaryotic tRNA synthetases.[22] Thus, the combination of the tRNA and the tRNA synthetase variant with highly orthogonal specificity is available for eukaryotic translation systems.[22−25] The DNA templates (104-mer, tRNA104**z** and tRNA104T) of the *E. coli* tRNA^{Tyr} with a CU**s** or CUA anticodon for T7 transcription were chemically synthesized, using the amidite of **z**. As the complementary base opposite **z** in the duplex DNA template of tRNA104**z**, A was introduced into the nontemplate strand. In addition, the last two nucleosides (G and T) at the 5′-termini of the template strand were replaced with their 2′-*O*-methylribonucleosides, which can reduce the addition of one or more nontemplated nucleotides at the 3′-terminus of the nascent transcript.[26] Transcription was performed with 3 mM **s**TP, 1 mM natural NTPs, 10 mM GMP, and [α-^{32}P]-ATP or [α-^{32}P]GTP, using 1 μM template, for 6 h at 37 °C (Figure 3b). The transcription efficiency for the synthesis of the tRNA with the CU**s** anticodon was as high as that for the control synthesis of the tRNA with the CUA anticodon (data not shown).

Internally labeled tRNA transcripts were isolated by gel electrophoresis and digested to nucleoside 3′-phosphates by RNase T_2. The labeled nucleoside 3′-phosphates were analyzed by 2D-TLC, as mentioned above (Figure 3c and Table 2). As shown in Figure 3c and Table 2, these data confirmed the site-specific incorporation of **s**TP into the anticodon of the tRNA by T7 transcription mediated by the **s**-**z** pairing. The nucleotide-composition analysis indicated that **s**TP was incorporated at position 36 in the tRNA opposite **z** in the template, and the misincorporation of **s**TP opposite the natural bases was negligible. In the presence of **s**TP, only the [α-^{32}P]ATP-labeled transcript obtained from the template, tRNA104**z**, gave a spot corresponding to the ribonucleoside 3′-phosphate of **s** (denoted

(22) Kiga, D.; Sakamoto, K.; Kodama, K.; Kigawa, T.; Matsuda, T.; Yabuki, T.; Shirouzu, M.; Harada, Y.; Nakayama, H.; Takio, K.; Hasegawa, Y.; Endo, Y.; Hirao, I.; Yokoyama, S. *Proc. Natl. Acad. Sci. U.S.A.* **2002**, *99*, 9715.
(23) Sakamoto, K.; Hayashi, A.; Sakamoto, A.; Kiga, D.; Nakayama, H.; Soma, A.; Kobayashi, T.; Kitabatake, M.; Takio, K.; Saito, K.; Shirouzu, M.; Hirao, I.; Yokoyama, S. *Nucleic Acids Res.* **2002**, *30*, 4692.
(24) Chin, J. W.; Cropp, T. A.; Anderson, J. C.; Mukherji, M.; Zhang, Z.; Schultz, P. G. *Science* **2003**, *301*, 964.
(25) Köhrer, C.; Yoo, J.-H.; Bennett, M.; Schaack, J.; RajBhandary, U. L. *Chem. Biol.* **2003**, *10*, 1095.
(26) Kao, C.; Rüdisser, S.; Zheng, M. *Methods* **2001**, *23*, 201.

by **s**p) (Figure 3c). Since the incorporated **s** became the 5′-neighbor of A, the 3′-phosphate of **s** was labeled with only [α-^{32}P]ATP, and the **s**p spot was detected by 2D-TLC. Thus, no spot corresponding to **s**p was observed on the 2D-TLC of the [α-^{32}P]GTP-labeled transcript from tRNA104**z** with **s**TP. As a control, the transcripts from the template consisting of the natural bases, tRNA104T, did not yield the **s**p spot on the 2D-TLC, even in the presence of **s**TP. From the nucleotide-composition analysis, the incorporation selectivity of **s** opposite **z** was 96% (Table 2, entry 11). Although the values of the misincorporations of **s**TP opposite the natural bases were 0.05−0.09 (Table 2, entries 13, 14, and 16), these misincorporations correspond to only 0.3−0.5% per position in the transcripts, as determined by the following formula: [**s** composition]/[total numbers of nucleotides as 5′ neighbors of A or G] × 100 (%).

In contrast to the high selectivity of the **s** incorporation opposite **z** into RNA, the **z** incorporation opposite **s** was less selective than the **y** incorporation opposite **s** by T7 RNA polymerase; the incorporation fidelity of **z**TP opposite **s** was only 50−70% (data not shown). This tendency also appeared in the single-nucleotide insertion experiments with the Klenow fragment, as mentioned above; the **z** incorporation efficiency opposite **s** into DNA was 10-fold lower than the **s** incorporation efficiency opposite **z** (Table 1, entries 1 and 6). This difference in the incorporation efficiencies mainly depends on the complex stabilities among the substrate, the template, and the polymerase; the K_m value of **z** incorporation opposite **s** (K_m = 600 μM) was much larger than that of **s** incorporation opposite **z** (K_m = 95 μM). This suggests that the low hydrophobicity and low stacking ability of **z** reduced the affinity between the **z** substrate and the polymerases. This is quite consistent with the fact that unnatural hydrophobic bases show good potential as substrates in single-nucleotide insertion experiments with the Klenow fragment.[8−11] Consequently, the **z** base can be unidirectionaly used as a template base, instead of **y**, for **s** incorporation into RNA.

In addition to the practical use of the **s**-**z** pair, these studies provide valuable information for understanding the mechanisms of replication and transcription. The differences in the selectivity between the **s**-**z** and **s**-**y** pairs in replication and transcription highlight the importance of the steric interactions between pairing bases. The bulky thienyl group of **s** efficiently excludes the pairing with the natural pyrimidine bases in transcription, but the pyrimidine-like base, **y**, tends to pair with the natural purine bases, as well as **s**, because of their favorable shape complementarity. In contrast, the five-membered ring of **z** does not fit as well with the natural purines, unlike **s**, and the specificity of the **s** incorporation into DNA and RNA opposite **z** is higher than that opposite **y**. This relationship between the steric interaction and the incorporation specificity has been found in other unnatural base pairs. For example, a hydrophobic five-membered ring, pyrrole-2-carbaldehyde (**Pa**), preferred another hydrophobic base, 9-methylimidazo[(4,5)-b]pyridine (**Q**), rather than the natural A or G, as a pairing partner in replication, but a hydrophobic six-membered ring, 2,4-difluorotoluene (**F**), preferred both **Q** and A.[27] The incomplete shape complementarity between the five-membered-ring bases and the natural purine bases is less favorable for removing the solvating waters on the purine bases. Interestingly, the addition of an acetyl group at position 4 of **z** improved the shape fitting between 4-acetyl-**z** and A, and d(4-acetyl-**z**)TP was efficiently incorporated into DNA opposite A by HIV reverse transcriptase.[28] Similarly, the bulky thienyl group at position 6 of **s** can also fill the space between **s** and **z**. In contrast to the fitting between A and 4-acetyl-**z** or A and **y**, the noncognate pairs between the natural purines and **z** or **s** and the natural pyrimidines exhibit poor shape complementarity, resulting in the high specificity of the **s**-**z** pairing in replication and especially in transcription.

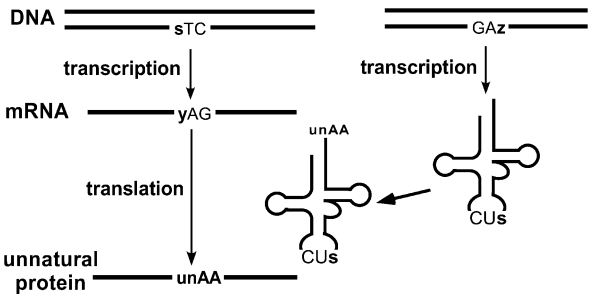

Figure 4. Two-unnatural-base-pair system mediated by the **s**-**y** and **s**-**z** pairs for the site-specific incorporation of amino acid analogues into proteins at desired positions. In the system, mRNA containing **y** and tRNA containing **s** were obtained from DNA templates containing **s** and **z**, respectively. unAA means an unnatural amino acid.

In this study, we have achieved the site-specific incorporation of **s**TP into RNA by T7 transcription mediated by the **s**-**z** pair. The five-membered ring of the **z** base effectively excludes the pairing with the natural purine bases. In combination with the **s**-**y** pair, the **s**-**z** pair can be applied to a coupled transcription−translation system,[15] in which the extra codon−anticodon interaction is created by the **s**-**y** pair; the transcription mediated by the **s**-**y** pairing generates mRNAs containing **y**, and the transcription mediated by the **s**-**z** pairing produces tRNAs containing **s** (Figure 4). This two-unnatural-base-pair system can be combined with the orthogonal tRNA-aminoacyl tRNA synthetase for amino acid analogues,[22−25] providing a convenient and powerful method for the site-specific incorporation of amino acid analogues into proteins at desired positions. Furthermore, the nucleoside of **s** exhibited a fluorescence emission centered at 430 nm, characterized by two major excitation maxima (299 and 352 nm), and its fluorescence quantum yield was 0.41 at pH 7.0. Thus, the **s**-**z** pair will also enable the site-specific fluorescent labeling of RNA fragments by T7 transcription.

Materials and Methods

General. Reagents and solvents were purchased from standard suppliers and were used without further purification. Reactions were monitored by thin-layer chromatography (TLC) using 0.25 mm silica gel 60F_{254} plates (Merck). ^{1}H NMR (270 MHz), ^{13}C NMR (68 MHz), and ^{31}P NMR (109 MHz) spectra were recorded on a JEOL EX270 magnetic resonance spectrometer. Purification of nucleosides was performed on a Gilson HPLC system with a preparative C18 column (Waters Microbond Sphere, 150 × 19 mm). Triphosphates were purified on a DEAE-Sephadex A-25 column (300 × 15 mm), and the final purification was achieved by a Gilson HPLC system with an analytical column (Synchropak RPP, 250 × 4.6 mm, Eichrom Technologies). High-resolution mass spectra (HRMS) and electrospray ionization mass spectra (ESI-MS) were recorded on a JEOL HX-110 or JM-700 mass spectrometer and a Waters micromass ZMD 4000, equipped with a Waters 2690 LC system, respectively.

(27) Mitsui, T.; Kitamura, A.; Kimoto, M.; To, T.; Sato, A.; Hirao, I.; Yokoyama, S. *J. Am. Chem. Soc.* **2003**, *125*, 5298.

(28) Kalman, T. I.; Sen, K.; Jiang, X.-J. *Nucleosides Nucleotides* **1999**, *18*, 847.

Synthesis of 1-(2-Deoxy-β-D-ribofuranosyl)imidazolin-2-one (2). A mixture of imidazolin-2-one[29] (505 mg, 6 mmol), hexamethyldisilazane (HMDS) (20 mL, 20 mmol), ammonium sulfate (60 mg, 0.45 mmol), and dichloroethane (5 mL) was refluxed for 2 h, and then the excess HMDS and dichloroethane were removed from the mixture by evaporation. The residue was dissolved in acetonitrile (10 mL), and the solution was mixed with an acetonitrile solution (10 mL) containing 1-chloro-2-deoxy-3,5-di-*O*-toluoyl-α-D-erythropentofuranose (1.56 g, 4 mmol). To the mixture was added a solution of $SnCl_4$ (0.1 mL, 0.85 mmol) in acetonitrile (5 mL) dropwise at −15 °C, and the solution was stirred for 1 h at room temperature. The reaction mixture was poured onto a dichloromethane (100 mL) and saturated $NaHCO_3$ solution (100 mL). The organic layer was washed with a saturated sodium chloride solution (100 mL), dried with $MgSO_4$, and evaporated in vacuo. The product was purified by silica gel column chromatography to give the fully protected mixture of α- and β-isomers (1.31 g, 75%). The mixture was dissolved in methanolic ammonia (100 mL), stirred for 12 h at room temperature, and evaporated. The residue was dissolved in H_2O, and each isomer (β-isomer, 155 mg; α-isomer, 193 mg) was separated by reversed-phase HPLC (Waters Microbond Sphere model C18, with a gradient from 0% to 7.5% (15 min) CH_3CN in H_2O).

1-(2-Deoxy-3,5-di-*O*-tetraisopropyldisiloxanyl-β-D-ribofuranosyl)-imidazolin-2-one. To a stirred solution of **2** (73 mg, 0.36 mmol) in DMF (1.8 mL) and pyridine (278 μL) in an ice-cold bath was added 1,3-dichloro-1,1,3,3-tetraisopropyldisiloxane (111 μL, 0.36 mmol). The reaction mixture was stirred at room temperature for 12 h and was partitioned with 5% $NaHCO_3$ and EtOAc. The organic layer was washed with 5% $NaHCO_3$ followed by saturated NaCl, dried over Na_2SO_4, and concentrated in vacuo. The product (120 mg, 78%) was purified from the residue by silica gel column chromatography (2% MeOH in CH_2Cl_2).

1-(2-Deoxy-3,5-di-*O*-tetraisopropyldisiloxanyl-β-D-ribofuranosyl)-2-diphenylcarbamoyloxyimidazole. To a stirred solution of 1-(2-deoxy-3,5-di-*O*-tetraisopropyldisiloxanyl-β-D-ribofuranosyl)imidazolin-2-one (120 mg, 0.27 mmol) and diphenylcarbamoyl chloride (150 mg, 2.4 equiv) in pyridine (2.7 mL) was added *N*,*N*-diisopropylethylamine (57 μL, 1.2 equiv). The solution was stirred at room temperature for 12 h and was partitioned with CH_2Cl_2 and water after the addition of MeOH. The organic layer was washed with 5% $NaHCO_3$ three times, dried over Na_2SO_4, and concentrated in vacuo. The product (100 mg, 60%) was purified from the residue by silica gel column chromatography (1% MeOH in CH_2Cl_2).

1-(2-Deoxy-β-D-ribofuranosyl)-2-diphenylcarbamoyloxyimidazole (3). To a stirred solution of 1-(2-deoxy-3,5-di-*O*-tetraisopropyldisiloxanyl-β-D-ribofuranosyl)-2-diphenylcarbamoyloxyimidazole (100 mg, 0.16 mmol) in THF (1.6 mL) was added 1 M TBAF in a THF solution (0.24 mL, 1.5 equiv). The reaction mixture was stirred at room temperature for 30 min and was partitioned with EtOAc and water. The organic layer was washed with saturated NaCl, dried over Na_2SO_4, and concentrated in vacuo. The product (60 mg, 96%) was purified by silica gel column chromatography (5% MeOH in CH_2Cl_2).

1-[2-Deoxy-5-*O*-(4,4′-dimethoxytrityl)-β-D-ribofuranosyl]-2-diphenylcarbamoyloxyimidazole. A quantity of 1-(2-deoxy-β-D-ribofuranosyl)-2-diphenylcarbamoyloxyimidazole (60 mg, 0.15 mmol) was coevaporated with dry pyridine three times. The residue was dissolved in pyridine (1.5 mL) with 4,4′-dimethoxytrityl chloride (52 mg, 1.0 equiv), and the solution was stirred at room temperature for 12 h. Water was added to the solution, and the product was extracted with EtOAc. The organic layer was washed with 5% $NaHCO_3$ twice and then with saturated NaCl, dried over Na_2SO_4, and concentrated in vacuo. The product was purified by silica gel column chromatography (2% MeOH in CH_2Cl_2) to give the dimethoxytrityl derivative (92 mg, 86%).

1-[2-Deoxy-5-*O*-(4,4′-dimethoxytrityl)-β-D-ribofuranosyl]-2-diphenylcarbamoyloxyimidazole 2-Cyanoethyl-*N*,*N*′-diisopropylamino-phosphoramidite (4). A quantity of 1-[2-deoxy-5-*O*-(4,4′-dimethoxytrityl)-β-D-ribofuranosyl]-2-diphenylcarbamoyloxyimidazole (92 mg, 0.13 mmol) was coevaporated with dry pyridine and dry THF three times each, and was dissolved in THF (650 μL). To the solution were added diisopropylethylamine (34 μL, 1.5 equiv) and 2-cyanoethyl-*N*,*N*′-diisopropylamino-chlorophosphoramidite (44 μL, 1.5 equiv). The reaction mixture was stirred at room temperature for 1 h. After the addition of MeOH (50 μL), the mixture was diluted with EtOAc/TEA (10 mL, 20:1, v/v). The mixture was washed with 5% $NaHCO_3$, followed by saturated NaCl three times. The organic layer was dried over Na_2SO_4 and concentrated in vacuo. The product was purified on a silica gel column, which was eluted with hexane:EtOAc (3:2, v/v) containing 2% TEA, to give the amidite (100 mg, 86%).

Synthesis of 1-(2-Deoxy-β-D-ribofuranosyl)imidazolin-2-one 5′-Triphosphate (dzTP, 5) and 1-(β-D-Ribofuranosyl)imidazolin-2-one 5′-Triphosphate (zTP). The ribonucleoside of **z** was synthesized according to the literature procedure.[17] To a solution of the 2′-deoxyribonucleoside of **z** or the ribonucleoside of **z** (0.1 mmol) and a proton sponge (33 mg, 0.15 mmol), in trimethyl phosphate (500 μL), was added $POCl_3$ (12 μL, 0.13 mmol) at 0 °C.[30] The reaction mixture was stirred at 0 °C for 2 h (for the 2′-deoxyribonucleoside of **z**), or for 6 h (for the ribonucleoside of **z**). Tri-*n*-butylamine (120 μL, 0.5 mmol) was added to the reaction mixture, followed by 0.5 M bis(tributylammonium)-pyrophosphate in a DMF solution (1.0 mL, 0.5 mmol). After 5 min, the reaction was quenched by the addition of 0.5 M triethylammonium bicarbonate (TEAB, 500 μL). The resulting crude product was purified by DEAE Sephadex A-25 column chromatography (eluted by a linear gradient of 50 mM to 1 M TEAB), and then by C18-HPLC (eluted by a gradient of 0% to 30% CH_3CN in 100 mM triethylammonium acetate).

Thermal Denaturation. The absorbance at 260 nm of the DNA fragments was monitored as a function of temperature (15−65 °C) on a Beckman DU650 spectrophotometer. The duplexes of 5′-GGTAAC-NATGCG and 5′-CGCATN′GTTACC (N = **s** or natural bases and N′ = **z**, **y**, or natural bases) were dissolved in 10 mM sodium phosphate (pH 7.0), 100 mM NaCl, and 0.1 mM EDTA, to give a duplex concentration of 5 μM. T_m values were calculated by the first derivatives of the melting curves.

Single-Nucleotide Insertion Experiments. Steady-state kinetics for single-nucleotide insertions were carried out according to the literature,[31,32] using the templates shown in Table 1. Primers were 5′-labeled by using [γ-^{32}P]ATP and T4 polynucleotide kinase. Primer-template duplexes (10 μM) were annealed, in a buffer containing 100 mM Tris-HCl (pH 7.5), 20 mM $MgCl_2$, 2 mM DTT, and 0.1 mg/mL bovine serum albumin, by heating at 95 °C and slow-cooling to 4 °C. The duplex solution (5 μL) was mixed with 2 μL of a solution containing the exonuclease-deficient Klenow fragment (Amersham USB, OH) diluted in a buffer containing 50 mM potassium phosphate (pH 7.0), 1 mM DTT, and 50% glycerol, and was incubated at 37 °C for more than 2 min. Reactions were initiated by adding 3 μL of a dNTP solution to the DNA−enzyme mixture at 37 °C. The amount of polymerase used (5−50 nM), the reaction time (1−20 min), and the gradient concentration of dNTP (0.6−2400 μM) were adjusted to give reaction extents of 25% or less. Reactions were quenched by adding 10 μL of a dye solution containing 0.05% BPB, 89 mM Tris−borate, 2 mM EDTA, and 10 M urea, and the mixtures were immediately heated at 75 °C for 3 min. The products were analyzed on a 15−20% polyacrylamide gel containing 7 M urea. The reaction extents were measured with a Bio-imaging analyzer (Fuji BAS 2500). Relative velocities (v_0) were calculated as the extents of the reaction divided by the reaction time, and were normalized to the enzyme concentration (20 nM) for the various enzyme concentrations used. The kinetic

(29) Hilbert, G. E. *J. Am. Chem. Soc.* **1932**, *54*, 3413.

(30) Kovács, T.; Ötvös, L. *Tetrahedron Lett.* **1988**, *29*, 4525−4528.

(31) Petruska, J.; Goodman, M. F.; Boosalis, M. S.; Sowers, L. C.; Cheong, C.; Tinoco, I. *Proc. Natl. Acad. Sci. U.S.A.* **1988**, *85*, 6252.

(32) Goodman, M. F.; Creighton, S.; Bloom, L. B.; Petruska, J. *Crit. Rev. Biochem. Mol. Biol.* **1993**, *28*, 83.

parameters (K_m and V_{max}) were obtained from Hanes−Woolf plots of [dNTP]/v_0 against [dNTP]. Each parameter was averaged from 3−4 data sets.

T7 Transcription. Templates (10 μM) were annealed in 10 mM Tris-HCl buffer (pH 7.6) containing 10 mM NaCl, by heating at 95 °C for 3 min and cooling to 4 °C. Transcription was carried out in 40 mM Tris-HCl buffer (pH 8.0) (20 μL) containing 24 mM $MgCl_2$, 2 mM spermidine, 5 mM DTT, 0.01% Triton X-100, 10 mM GMP, 1 mM each NTP, 0−3 mM **s**TP, 2 μCi [α-^{32}P]UTP (Amersham), 2 μM template, and 50 units of T7 RNA polymerase (Takara Shuzo, Kyoto, Japan). The addition of GMP reduced the production of the full-length +1 product yielded by the random incorporation of an uncoded extra base, and facilitated the analysis.[33] After incubation for 3 h at 37 °C, the reaction was quenched by the addition of 20 μL of the dye solution. This mixture was heated at 75 °C for 3 min, and then was loaded onto a 20% polyacrylamide−7 M urea gel. The transcription products were eluted from the gel with water, and were precipitated with ethanol. The transcripts were digested by 0.75 unit of RNase T_2 at 37 °C for 90 min, in 10 μL of 15 mM sodium acetate buffer (pH 4.5) and 0.05 A_{260} unit of *Escherichia coli* tRNA. The digestion products were analyzed by 2D-TLC using a Merck HPTLC plate (100 × 100 mm) (Merck, Darmstadt, Germany) with the following developing solvents: isobutyric acid−ammonia−water (66:1:33 v/v/v) for the first dimension, and isopropyl alcohol−HCl−water (70:15:15 v/v/v) for the second dimension. The products on the gels and the TLC plates were analyzed with the Bio-imaging analyzer.

For the tRNA synthesis, the template strand (5′-TmGmGTG-GTGGGGGAAGGATTCGAACCTTCGAAGTCGATGACGGCAG-ATTN [N = **z** or T] AGAGTCTGCTCCCTTTGGCCGCTCGG-GAACCCCACCTATAGTGAGTCGTATTATC [denoted by tRNA104**z** (N = **z**) and tRNA104T (N = T), where Tm = 2′-*O*-methylthymidine and Gm = 2′-*O*-methylguanosine], 10 μM) and the nontemplate strand (5′-GATAATACGACTCACTATAGGTGGGGTTCCCGAGCGGC-CAAAGGGAGCAGACTCTAAATCTGCCGTCATCGACTTCGAAG-GTTCGAATCCTTCCCCCACCACCA, 10 μM) were annealed in 10 mM Tris-HCl buffer (pH 7.6) containing 10 mM NaCl, by heating at 90 °C for 3 min and cooling to 4 °C at a rate of 0.3 °C/sec. Transcription was carried out in 40 mM Tris-HCl buffer (pH 8.0) (20 μL) with 24 mM $MgCl_2$, 2 mM spermidine, 5 mM DTT, 0.01% Triton X-100, 10 mM GMP, 1 mM each NTP, 0 or 3 mM **s**TP, 2 μCi of [α-^{32}P]ATP or [α-^{32}P]GTP, 1 μM template, and 50 units of T7 RNA polymerase. After incubation for 6 h at 37 °C, the reaction was quenched by the addition of 20 μL of the dye solution. This mixture was heated at 75 °C for 3 min, and then was loaded onto a 10% polyacrylamide−7 M urea gel. The transcripts were eluted from the gel with water, and were precipitated with ethanol. The transcripts were digested by 1.5 units of RNase T_2 in 10 μL of 15 mM sodium acetate buffer (pH 4.5), containing 0.05 A_{260} unit of *E. coli* tRNA, at 37 °C overnight. The digestion products were analyzed by 2D-TLC, as mentioned above.

Acknowledgment. This work was supported by the RIKEN Structural Genomics/Proteomics Initiative (RSGI), the National Project on Protein Structural and Functional Analyses, Ministry of Education, Culture, Sports, Science and Technology of Japan, and by a Grant-in-Aid for Scientific Research (KAKENHI 15350097) from the Ministry of Education, Culture, Sports, Science, and Technology.

Supporting Information Available: NMR and MS data for **2**−**5** and NMR charts for the characterization of the nucleoside derivatives of **z** (**2**). This material is available free of charge via the Internet at http://pubs.acs.org.

JA047201D

(33) Ohtsuki, T.; Kimoto, M.; Ishikawa, M.; Mitsui, T.; Hirao, I.; Yokoyama, S. *Proc. Natl. Acad. Sci. U.S.A.* **2001**, *98*, 4922.